REFLECTANCE AND ALBEDO, SURFACE

J A Coakley, Oregon State University, Corvallis, OR, USA

Introduction

'Albedo' is Latin, meaning whiteness. The albedo of a surface is the fraction of the incident sunlight that the surface reflects. Radiation that is not reflected is absorbed by the surface. The absorbed energy raises the surface temperature, evaporates water, melts and sublimates snow and ice, and energizes the turbulent heat exchange between the surface and the lowest layer of the atmosphere. The surface albedo is a key ingredient in the remote sensing of surface and atmospheric properties from space. The spectral and angular dependence of reflected sunlight is used to infer surface properties such as the extent and nature of vegetation cover. It must also be allowed for when determining atmospheric composition such as the amount, size, and optical properties of haze particles. Over continents, the largest component of the reflected sunlight under cloud-free conditions is due to reflection by the surface. Consequently, the determination of atmospheric composition from reflected sunlight requires accurate knowledge of the contribution made by the reflecting surface.

Different surfaces have different albedos. Oceans, lakes, and forests reflect relatively small fractions of the incident sunlight and have low albedos. Snow, sea ice, and deserts reflect relatively large fractions of the incident sunlight and have large albedos. While estimates of albedos for various surfaces are presented later (**Table 3**), it should be recognized that an albedo is not an intrinsic property of a surface. Instead, for any surface, the albedo depends on the spectral and angular distributions of the incident light, which in turn are governed by atmospheric composition and the direction of the beam of light from the sun.

Ideally, surfaces may be broken into components, each component reflecting light following its own intrinsic optical rules for the wavelength and angular dependence of reflection. In practice, however, when viewed at the few-meters to several-kilometers resolution typical of spaceborne sensors, surfaces exhibit complex mixtures of components and geometric structures. At such scales, surfaces can contain any mixture of soil, vegetation, twigs, branches, rocks, snow, ice, water, and so on. The list is seemingly endless. Even if the scene is spatially uniform, reflection by the individual surface elements, such as grains of sand in a desert, or snowflakes in a drift, can be so difficult to treat according to the principles of optics as to render predictions of reflectance futile. In addition, topography and the consequent shading add further to the complexity. Thus, for practical treatments, surfaces are reduced to having few components, even as few as one or two, and both the spectral and angular distributions of the reflectances for the individual components are highly simplified.

Simplifications of the spectral dependence of surface reflection are often dealt with through use of wavelength intervals over which the reflectivity of the surface remains reasonably constant. Simplifications of the angular dependence of surface reflection are often dealt with through the separation of the incident light into two components: one for the direct beam of incident light, which is the sunlight that has not been absorbed or scattered in the atmosphere; and one for incident sunlight that has been scattered into directions that differ markedly from that of the direct beam. These simplifications are used below in combination with a global inventory of surface types to produce global maps of surface albedos. These maps, however, should be taken as providing only rudimentary estimates. Because of the complexities noted earlier, systematic attempts to construct global maps of surface albedos from satellite observations are just now being undertaken.

Physical Processes that Shape the Surface Albedo

Insight into the spectral and angular dependence of surface reflection can be gained by considering a few fundamental principles. To begin, light is reflected at interfaces between media with distinct indices of refraction. If the media and the surface dividing the media have properties which are spatially uniform over scales large enough for individual surface elements to be treated as planar then the reflection is described by Fresnel's laws. The angle of reflection for a particular surface element is equal to the angle of incidence. The fraction of reflected light depends on wavelength according to the optical properties of the two media.

Many surfaces in nature, on the other hand, are composed of elements that have scales comparable to the wavelength of the incident light, such as grains of soil and sand, snowflakes, air bubbles in ice, etc. In principle, reflectances for such surfaces can be arrived

at through radiative transfer calculations. The reflected radiances adopt an angular pattern that is typical of light that has suffered multiple scatterings. Multiple scattering patterns also arise for surface elements that are spatially uniform, such as the leaf of a plant, but each element, through its orientation with respect to the incident light, may reflect light differently from similar elements nearby. If the elements are not strongly absorbing, then light reflected by one surface element may be reflected by another. Likewise, with Fresnel reflection, if the interface is spatially varying then reflection from one portion of the surface may be reflected by another portion. However, if a surface element is strongly absorbing, then the reflection approximates single scattering. For single scattering, the angular distribution of the reflected light can be described in terms of a single angle, the scattering angle. Multiple scattering and multiple reflection give rise to reflected light that cannot be described in terms of a single angle.

Figure 1 illustrates the conventions used here to specify the directions of the incident and reflected light. In the figure, light from the sun is shown to be incident on a surface in the XY plane. The incident sunlight is taken to be in the YZ plane. The orientation of the axes is arbitrary, and positioning the axes with the incident sunlight in the YZ plane places no restrictions on the outcome. The angle between the direction to the sun and the normal to the surface is referred to as the solar zenith angle, θ_0. The view zenith angle, θ, is the angle between the direction of the observer and the normal to the surface. The relative azimuth angle, ϕ, is the angle between the direction of the incident sunlight and the direction of the reflected light when projected in the plane containing the reflecting surface, the XY plane. In Figure 1, the relative azimuth angle is 0° for an observer facing the sun and 180° for an observer with their back to it. This convention for the relative azimuth angle is often used for radiative transfer in the atmosphere. The convention is opposite that often used in the description of land surface processes. In describing land surfaces, the relative azimuth angle is often the angle between the observer and the sun: 180° with the observer facing the sun and 0° with the observer's back to the sun.

The geometry illustrated in Figure 1 also applies for an arbitrary source of light incident on the surface. For instance, scattered sunlight may strike the surface from a direction markedly different from that of the direct sunlight. Scattered light will have its own zenith angle, θ', and its own azimuth angle, ϕ', relative to the direction of the unscattered beam of light from the sun.

By definition, the spectral albedo, α_λ, which is the albedo for monochromatic radiation at wavelength λ,
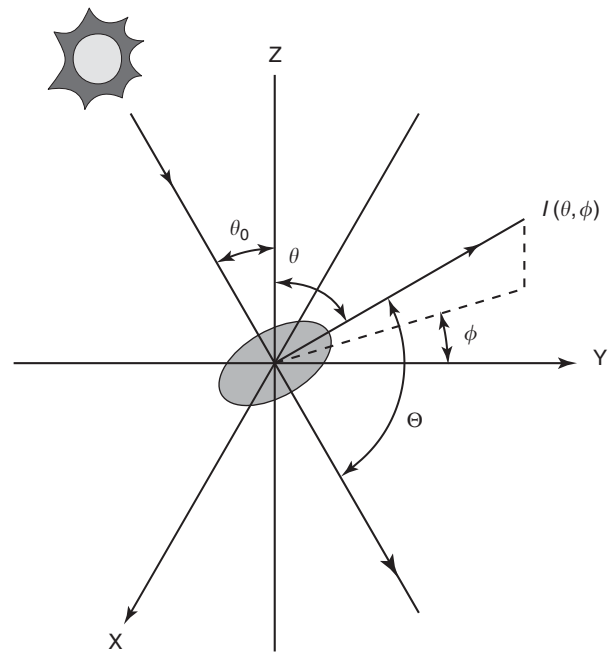
Figure 1 Orientation of incident sunlight and reflected light. θ_0 is the solar zenith angle, θ the view zenith angle, ϕ the relative azimuth angle, and Θ the scattering angle. The incident sunlight is taken to be in the YZ plane.

is given by

$$\alpha_\lambda = \frac{F_\lambda^+}{F_\lambda^-} \qquad [1]$$

where F_λ^- is the flux of light incident on the surface and F_λ^+ is the flux of light reflected by the surface. Radiative flux is the power per unit area per unit wavelength interval that is incident on or reflected by the surface. Radiative flux is often referred to as irradiance. The units of radiative flux are $W\,m^{-2}\,\mu m^{-1}$. The broadband albedo, or simply the albedo, is likewise given by the ratio of the total radiative fluxes,

$$\alpha = \frac{F^+}{F^-} \qquad [2]$$

where the integration over wavelength is performed separately for the incident and reflected radiative fluxes prior to taking the ratio. The total fluxes or total irradiances give the total radiative power per unit area incident on or reflected by the surface. The units of total radiative flux are $W\,m^{-2}$.

As mentioned in the introduction, the albedo gives the fraction of sunlight reflected by the surface. The fraction absorbed by the surface is thus given by the fraction not reflected, $(1 - \alpha)F^-$. It is this energy that raises the surface temperature, evaporates water, spawns turbulent exchange with the overlying atmosphere, etc.

The radiative fluxes, in turn, are given by the specific intensities. The specific intensities are often referred to as radiances. In terms of the incident and reflected radiances, $I_\lambda^\pm(\theta, \phi)$, the fluxes are given by

$$F_\lambda^\pm = \int_0^{2\pi} d\phi \int_0^{\pi/2} d\theta \, \sin \theta \, \cos \theta \, I_\lambda^\pm(\theta, \phi) \quad [3]$$

The specific intensity is the radiative power per unit area per unit wavelength per unit solid angle flowing through a surface perpendicular to the direction of propagation (Goody and Young 1989). The solid angle associated with the radiance is the angle that the area for which the radiance is defined subtends at the source of the light. The solid angle arises because light propagates in a straight line after leaving its source and the source is taken to be at a point. Consequently, the intensity falls as the inverse of the square of the distance from the source, and this dependence is carried by the solid angle. The increment of solid angle in eqn [3] is given by $d\Omega = \sin \theta \, d\theta \, d\phi$. The $\cos \theta$ factor in [3] accounts for the projection of the area for which the radiance is defined onto the surface for which the radiative flux is defined. This projection is equivalent to projecting the shade of the area associated with the radiance onto the area associated with the flux.

The first approximation to surface reflection is that the surface reflects isotropically. That is, the reflected intensity is independent of view zenith and relative azimuth angles, and is simply related to the incident flux. From eqn [3], for isotropic reflection, $F_\lambda^+ = \pi I_\lambda^+$, and consequently,

$$I_\lambda^+ = \frac{\alpha_\lambda F_\lambda^-}{\pi}$$

Such a surface is called Lambertian. No surface is truly Lambertian. Those that come closest are extensive fields of snow and ice. Snow and ice absorb little sunlight at visible wavelengths. As a result, multiple scattering is possible. The angular dependence of the reflected light is reduced as the number of scatterings increases. Even though isotropic reflection is not common, isotropic reflection is often adopted as an approximation because it simplifies estimates of the reflected intensities, I_λ^+.

Fresnel reflection describes the reflection of light at the boundary of two media with distinct indices of refraction when the media are uniform at all spatial scales, including length scales that are small compared with the wavelength of the light, and the surface separating the media can be taken to be a plane. For Fresnel reflection, the angle of reflection is equal to the angle of the incident light: the view zenith angle is equal to the zenith angle of the source, and the relative azimuth angle is zero for the direction of specular reflection. Fresnel reflection is often adopted for water and ice surfaces. To capture the undulation of water and ice surfaces, distributions are used for the orientation of the surface elements with respect to the direction of the incident light. The effect of a distribution of orientation is to produce a distribution of reflected intensities that peaks near the direction of specular reflection by a flat surface and falls with the angle measured with respect to the direction of specular reflection. For oceans, the bright pattern of reflected sunlight near the direction of specular reflection is referred to as sun glint.

In addition to Fresnel reflection, all surfaces, including water and ice, have internal elements with sizes comparable to the wavelengths of incident sunlight. These elements scatter light and contribute to the light reflected by the surface. In oceans, minuscule variations in density, air bubbles, particles of sand and dust, organic compounds, and microscopic organisms all give rise to scattered light. On land, the scattering is by grains of sand and particles of soil. If these internal elements absorb most of the incident light, then the reflected light can be approximated as being due to single scattering. The intensity of the reflected light becomes a function only of the scattering angle, which for the orientation illustrated in **Figure 1** is given by

$$\cos \Theta = \sin \theta \, \sin \theta_0 \, \cos \phi - \cos \theta \, \cos \theta_0 \quad [4]$$

The distribution of scattered light is specified in terms of a probability distribution function, referred to as a scattering phase function. $P(\Theta) \sin \Theta \, d\Theta/2$ is the fraction of the scattered radiation that has been scattered through scattering angle Θ and into an incremental ring of solid angle given by $d\Omega = 2\pi \sin \Theta \, d\Theta$. The phase function is defined so that it is unity for isotropic scattering, and it is normalized so that

$$\frac{1}{2} \int_0^\pi d\Theta \, \sin \Theta P(\Theta) = 1$$

Because the elements which give rise to the largest component of scattered light are often larger than the wavelength of the incident sunlight, the scattering is typically anisotropic. The Henyey–Greenstein phase function provides a convenient prescription for the distribution of light that is scattered anisotropically and is given by

$$P(g, \Theta) = \frac{1 - g^2}{(1 + g^2 - 2g \cos \Theta)^{3/2}} \quad [5]$$

where g is adjusted to give the proper degree of anisotropic scattering. g is referred to as the asymmetry parameter. It is the average cosine of the scattering angle and is given by

$$g = \langle \cos \Theta \rangle = \frac{1}{2} \int_0^\pi d\Theta \, \sin \Theta \, \cos \Theta P(g, \Theta) \quad [6]$$

For $g = 0$, the scattering is isotropic; for $g < 0$, most of the radiation is scattered in the direction of backscattering, toward an observer with their back to the source, and for $g > 0$, most of the radiation is scattered in the direction of forward scattering, toward an observer facing the source.

If absorption is not strong, light can be scattered more than once before it leaves a surface. Likewise, light reflected from one portion of a spatially varying surface can be reflected by another portion on its upward path towards the atmosphere. The simplest treatment of the multiply scattered component was offered by Minnaert, who attempted to fit reflectances observed for Mars. The reflectance was taken to be given by

$$\rho(\theta', \theta) = \rho_0 \, \cos^{k-1} \theta' \, \cos^{k-1} \theta$$

where k and ρ_0 are adjusted to give the observed reflectances. With multiply scattered and reflected light, the angular distribution is no longer a function of the scattering angle only.

The effects of single scattering, multiple scattering, and an additional refinement for light reflected in the backward direction, scattering angles near $180°$, have been bundled to form an empirical, analytic expression for surface reflectance. Following Rahman *et al.* (1993), reflection by a land surface is taken to be given by

$$\rho(\theta', \theta, \phi) = \rho_0 \frac{\cos^{k-1} \theta' \, \cos^{k-1} \theta}{(\cos \theta' + \cos \theta)^{1-k}} P(g, \Omega)$$

$$\times (1 + R(G, \Delta)) \quad [7]$$

where $P(g, \Omega)$ is the Henyey–Greenstein phase function given by [5] and

$$R(G, \Delta) = \frac{1 - \rho_0}{\Delta + G} \quad [8]$$

with

$$G(\theta', \theta, \phi)$$
$$= \sqrt{\tan^2 \theta' + \tan^2 \theta - 2 \tan \theta' \tan \theta \cos \phi}$$

In [7] ρ_0, k, g, and Δ are parameters that are adjusted to achieve the best agreement with observed reflectances. The reflectance, $\rho(\theta', \theta, \phi)$, is called the bidi-

rectional reflectance distribution function (BRDF). The function $R(G, \Delta)$ peaks sharply, depending on the value of Δ, in the direction of backscattered light, $\Theta = 180°$. It is included to treat the 'hot spot' or 'Heiligenschein' in the reflection pattern for land surfaces. The peak in reflectances arises as a result of the absence of shadows when the surface is viewed from the direction of backscattered light. The peak is often observed when looking out of the window of an airplane flying over land. With the sun on the opposite side of the plane, the peak surrounds the shadow of the plane as it appears on the land surface. In eqns [7] and [8], Δ is adjusted to fit the reflectance for the hot spot; otherwise, $\Delta = 1$ serves as a default value.

Figure 2 shows an example of the bidirectional reflectance distribution function for a homogeneous field of clover. In the diagram, the length of the radius represents the view zenith angle; the polar angle represents the relative azimuth angle. The reflectances are for incident light with a zenith angle of $45°$. The parameters used to obtain these reflectances are taken from Rahman *et al.* (1993) and are given in **Table 1** along with parameters for other surfaces. The parameters were derived by fitting [7] to observations of bidirectional reflectances. Only in the case of clover is the hot spot treated through an adjustment of the value of Δ.

In the field, surface albedo measurements are made using a combination of instruments, positioned either on tripods, of order 3 m in height, or on towers, of order 20 m or greater in height. The instruments include various combinations of spectral and broadband narrow-field-of-view radiometers to measure specific intensities and radiances integrated over all wavelengths, and spectral and broadband pyranometers to measure radiative fluxes and the radiative fluxes integrated over all wavelengths, or total radiative fluxes. The narrow-field-of-view radiometers provide information on the directional dependence of the incident and reflected light, while the pyranometers are used to measure the incident and reflected radiative fluxes. Often, one set of instruments is deployed to measure reflected radiances and irradiances, another to measure the incident flux. The difficulties that arise in measuring surface reflectances and albedos include the spatial heterogeneity of the surface, the spectral and angular responses of the various instruments, the radiometric calibration of the various instruments, and effects due to shading of the surface by the structure supporting the instruments. Despite the difficulties, careful measurements of surface albedo have been shown to be repeatable to within ± 0.02.

For the example shown in **Figure 2**, the reflectances were measured at visible wavelengths, 0.45–0.68 μm,
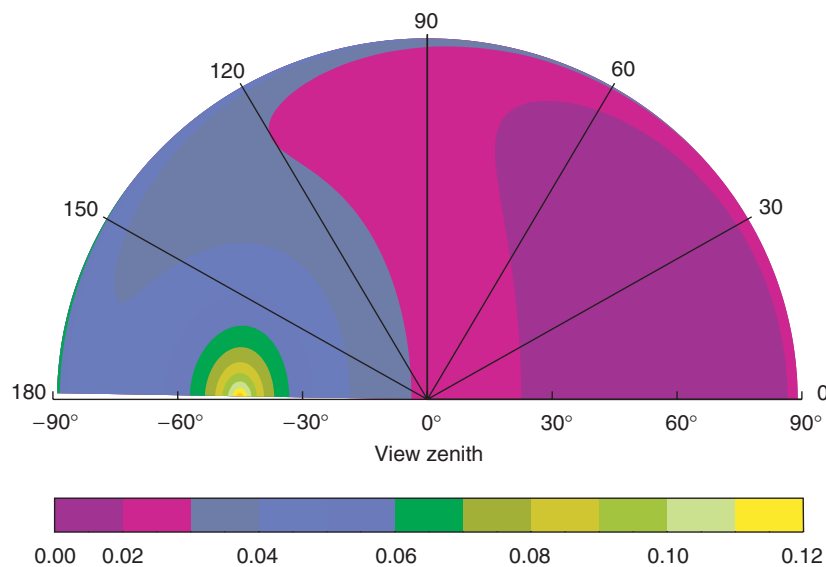
Figure 2 Bidirectional reflectance distribution function for visible wavelengths calculated for clover using eqn [7] and data from Rahman *et al.* (1993) as given in **Table 1**. The radial axis is the view zenith angle, the polar axis the relative azimuth angle. The solar zenith angle is 45°. The 'hot spot' is the peak in the reflectance at a view zenith angle of $-45°$, in the direction of backscattered light, relative azimuth angle of 180°.

and near-infrared wavelengths, 0.73–1.1 μm. The hot spot occurs at a view zenith angle of 45°, the zenith angle of the incident light. Most of the reflected light is distributed in the direction of backscattered radiation, $g < 0$. The parameters given in **Table 1** indicate that this is common for several land surface types.

Figure 3 shows the effect of multiple scattering on the surface reflectance for clover. The effect is revealed as different values of the BRDF for the same scattering angle, but different combinations of zenith angles for the incident light (as indicated by the different symbols), view zenith angles, and relative azimuth angles. The results suggest that for low sun (large zenith angle for the incident light), the scattering becomes more like that for single scattering.

Expressions like [7] appear to offer reasonable representations for the angular distribution of re-

flected light from surfaces. Such expressions are being used to construct global maps of surface albedos from multispectral and multi-angle satellite observations of land surfaces under cloud-free conditions. The goal is to characterize the surface albedo to within ± 0.05 or better in order to reliably estimate the surface energy budget. In addition, from the spectral and angular distribution of the reflected radiances, surface conditions are characterized in terms of, for example, the extent and type of vegetation, or the extent and depth of snow cover. Of course, to characterize the surface reflectance, the composition of the atmosphere must be determined for the times of observation. Atmospheric composition affects the spectral and angular distribution of the light incident on the surface, as well as the amount of light reflected by the surface that is attenuated by the atmosphere. Making corrections for

Table 1 Parameters for the bidirectional reflection distribution function given by [7] and [8]

Surface	Visible				Near Infrared			
	ρ_0	k	g	Δ	ρ_0	k	g	Δ
Plowed field	0.076	0.648	-0.290	1	0.095	0.668	-0.268	1
Grassland	0.183	0.780	-0.100	1	0.251	0.784	-0.083	1
Hard wheat	0.133	0.851	-0.114	1	0.211	0.718	$+0.086$	1
Lawn	0.026	0.536	-0.007	1	0.238	0.668	$+0.015$	1
Soybean	0.026	0.642	$+0.200$	1	0.357	0.879	-0.045	1
Coniferous forest	0.004	0.634	-0.142	1	0.058	0.525	-0.179	1
Savannah	0.019	0.868	-0.241	1	0.091	0.726	-0.156	1
Pasture land	0.013	0.679	-0.170	1	0.252	0.766	-0.033	1
Clover	0.011	0.706	-0.211	0.207	—	—	—	—

Data taken from Rahman *et al.* (1993).
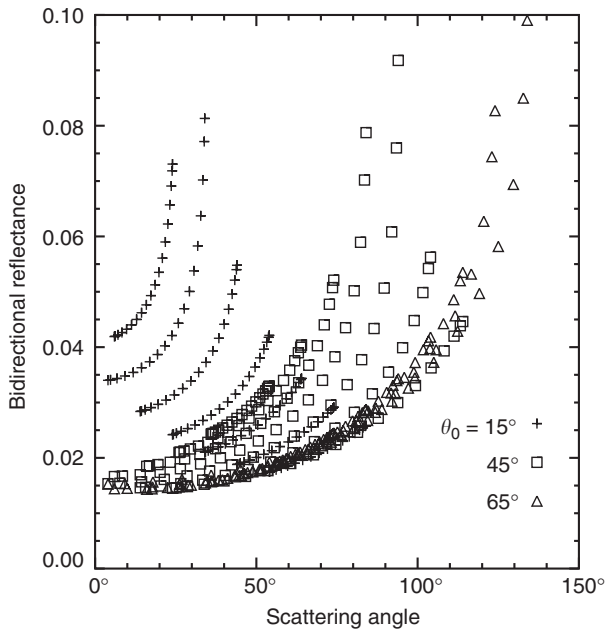
Figure 3 Bidirectional reflectance distribution function and scattering angle for clover. Reflectances are calculated using [7]. Values for a particular solar zenith angle are identified by the symbols.

atmospheric effects is a challenging problem for the remote sensing of surface reflectance.

Surface Albedo

The spectral and angular dependence of the surface reflectivity in eqns [1] and [7] are often simplified by (1) describing the spectral dependence in terms of wavelength intervals for which the surface reflectance is reasonably constant, and (2) dividing the angular distribution of the incident light into two components: a direct component composed of sunlight that has not been scattered or absorbed, referred to as the direct beam, and a diffuse component composed of sunlight that has undergone scattering and is incident with zenith angles that differ significantly from that of the direct beam. Following eqn [1], the albedo for the wavelength interval i is given by

$$\alpha_i = \frac{F_i^+}{F_i^-}$$

with the flux of radiation incident on the surface given by $F_i^- = F_{i\mathrm{DIR}}^- + F_{i\mathrm{DIF}}^-$, where $F_{i\mathrm{DIR}}^-$ is the flux of radiation incident on the surface due to sunlight that passes through the atmosphere without being scattered or absorbed, i.e., in the direction of the direct beam as specified by the solar zenith angle, and $F_{i\mathrm{DIF}}^-$ is the flux due to sunlight that is scattered as it passes through the atmosphere. Following Briegleb and

Ramanathan (1982), this diffuse radiation is often taken to be isotropic. Under such conditions, the surface albedo is specified in terms of a direct component, which depends on the solar zenith angle, and a diffuse component. Briegleb and Ramanathan suggest that the direct component of the surface albedo, $\alpha_i(\mu_0)$, be expressed in terms of the diffuse component, $\alpha_{i\mathrm{D}}$, as

$$\alpha_i(\mu_0) = \alpha_{i\mathrm{D}} \frac{1+d}{1+2d\mu_0} \qquad [9]$$

where $\mu_0 = \cos\theta_0$ is the cosine of the solar zenith angle, and θ_0 and d are adjusted to obtain the observed dependence of the surface albedo on solar zenith angle. In eqn [9], the direct and diffuse components of the albedo are made to be equal when the solar zenith angle is $60°$, clearly an approximation. In terms of the direct and diffuse albedos, the reflected flux is given by

$$F_i^+ = F_{i\mathrm{DIR}}^- \alpha_i(\mu_0) + F_{i\mathrm{DIF}}^- \alpha_{i\mathrm{D}} \qquad [10]$$

Note that both the direct and the diffuse fluxes incident on the surface depend on the solar zenith angle. Generally, for cloud-free conditions, the diffuse flux increases as the solar zenith angle increases. In addition, the downward diffuse flux incident on the surface is also a function of the surface albedo. Consistent with the approximations used here, the flux of diffuse radiation incident on the surface is given by

$$F_{i\mathrm{DIF}}^- = \frac{F_{i\mathrm{DIR}}^- \alpha_i(\mu_0) R_{i\mathrm{D}}}{1 - \alpha_{i\mathrm{D}} R_{i\mathrm{D}}} + \frac{F_{i\mathrm{DIF0}}^-}{1 - \alpha_{i\mathrm{D}} R_{i\mathrm{D}}}$$

where $R_{i\mathrm{D}}$ is the spherical albedo of the atmosphere when viewed from the surface and $F_{i\mathrm{DIF0}}^-$ is the diffuse downward flux for the case in which the surface albedo is zero. For cloud-free conditions at midlatitudes with an average continental aerosol having a $0.55\,\mu\mathrm{m}$ optical depth of 0.1, $R_{i\mathrm{D}}$ ranges from approximately 0.3 at $0.3\,\mu\mathrm{m}$ to approximately 0.03 at $0.9\,\mu\mathrm{m}$.

The diffuse components of the surface albedos are specified for five wavelength intervals in **Table 2** for various surface types. For land surfaces, each albedo is described by two components, one for the primary cover, typically a vegetative cover, and one for the secondary cover, typically bare soil. The albedo is obtained by linearly weighing the contributions of the two components. The fraction of the primary cover is given by f; the fraction of the secondary cover is given by $1 - f$. For arable land and deciduous forests, f is made to depend on season. Values of f and d for each surface type are given in **Table 3**. For snow and sea ice,

Table 2 Spectral dependence of the diffuse component of the albedo for various surfaces

	Primary surface				Secondary surface			
Wavelength interval (μm)	0.2–0.5	0.5–0.7	0.7–0.85	0.85–4.0	0.2–0.5	0.5–0.7	0.7–0.85	0.85–4.0
Mixed farming, tall grass	0.04	0.08	0.24	0.24	0.05	0.1	0.3	0.3
Tall/medium grassland, evergreen shrubland	0.05	0.10	0.30	0.30	0.08	0.17	0.25	0.35
Short, grassland, meadow and shrubland	0.03	0.04	0.20	0.20	0.05	0.1	0.15	0.22
Evergreen forest (needleleaved)	0.03	0.06	0.30	0.30	0.03	0.04	0.2	0.2
Mixed deciduous, evergreen forest	0.03	0.06	0.30	0.30	0.03	0.04	0.20	0.20
Deciduous forest	0.03	0.06	0.30	0.30	0.07	0.13	0.19	0.28
Tropical evergreen broadleaved forest	0.03	0.04	0.20	0.20	0.05	0.10	0.15	0.22
Medium/tall grassland, woodland	0.03	0.05	0.25	0.25	0.05	0.10	0.30	0.30
Desert	0.28	0.42	0.50	0.50	0.15	0.25	0.35	0.4
Tundra	0.04	0.10	0.25	0.25	0.07	0.13	0.19	0.28
Snow	0.76	0.76	0.325	0.325	–	–	–	–
Sea ice	0.75	0.70	0.50	0.50	–	–	–	–

Data taken from Briegleb *et al.* (1986) and Briegleb and Ramanathan (1982).

the albedo depends on the fraction of the area covered and the thickness of the snow and ice layers. In the case of snow, it also depends on the age of the snow. Albedos for fresh snow are higher than those for aged snow. The values in the table are intermediate between those for fresh and aged snow. For sea ice, the albedo can be reduced by the effects of melt ponds on the ice. The values in the table are for ice free of melt ponds. For water, the surface albedo is taken to be independ-

ent of wavelength and the albedo for direct radiation is taken to be given by (Briegleb *et al.*, 1986)

$$
\alpha(\mu_0) = \frac{0.026}{(\mu_0^{1.7} + 0.065)} + 0.15 \\
\times (\mu_0 - 0.1)(\mu_0 - 0.5)(\mu_0 - 1.0) \quad [11]
$$

The albedo for diffuse radiation is taken to be 0.06.

Table 3 Solar zenith angle correction factor, *d* in eqn [9], primary surface coverage, *f*, and broadband surface albedos for a solar zenith angle 60°

Surface	d	f		Albedo[a]	
		Summer	Winter	Summer	Winter
Mixed farming, tall grass	0.4	0.85	0.25	0.16	0.18
Tall/medium grassland, evergreen shrubland	0.4	0.8	0.7	0.20	0.21
Short, grassland, meadow and shrubland	0.4	0.8	0.7	0.21	0.20
Evergreen forest (needle leaved)	0.1	0.8	0.7	0.12	0.13
Mixed deciduous, evergreen forest	0.1	0.8	0.6	0.16	0.16
Deciduous forest	0.1	0.8	0.5	0.17	0.18
Tropical evergreen broadleaved forest	0.1	0.9	0.6	0.12	0.15
Medium/tall grassland, woodland	0.4	0.8	0.5	0.15	0.18
Desert	0.4	0.5	0.5	0.36	0.36
Tundra	0.1	0.4	0.3	0.17	0.17
Snow	0.0	–	–	0.66	0.66
Sea ice	0.0	–	–	0.62	0.62
Ocean	–	–	–	0.07	0.07

Data taken from Briegleb *et al.* (1986).
[a]Albedos were calculated for cloud-free conditions using midlatitude profiles of temperature, humidity, and ozone for summer and winter conditions. Values of the broadband surface albedo depend on seasonal surface coverage, *f*, solar zenith angle, and radiative properties of the atmosphere.

(A)

(B)
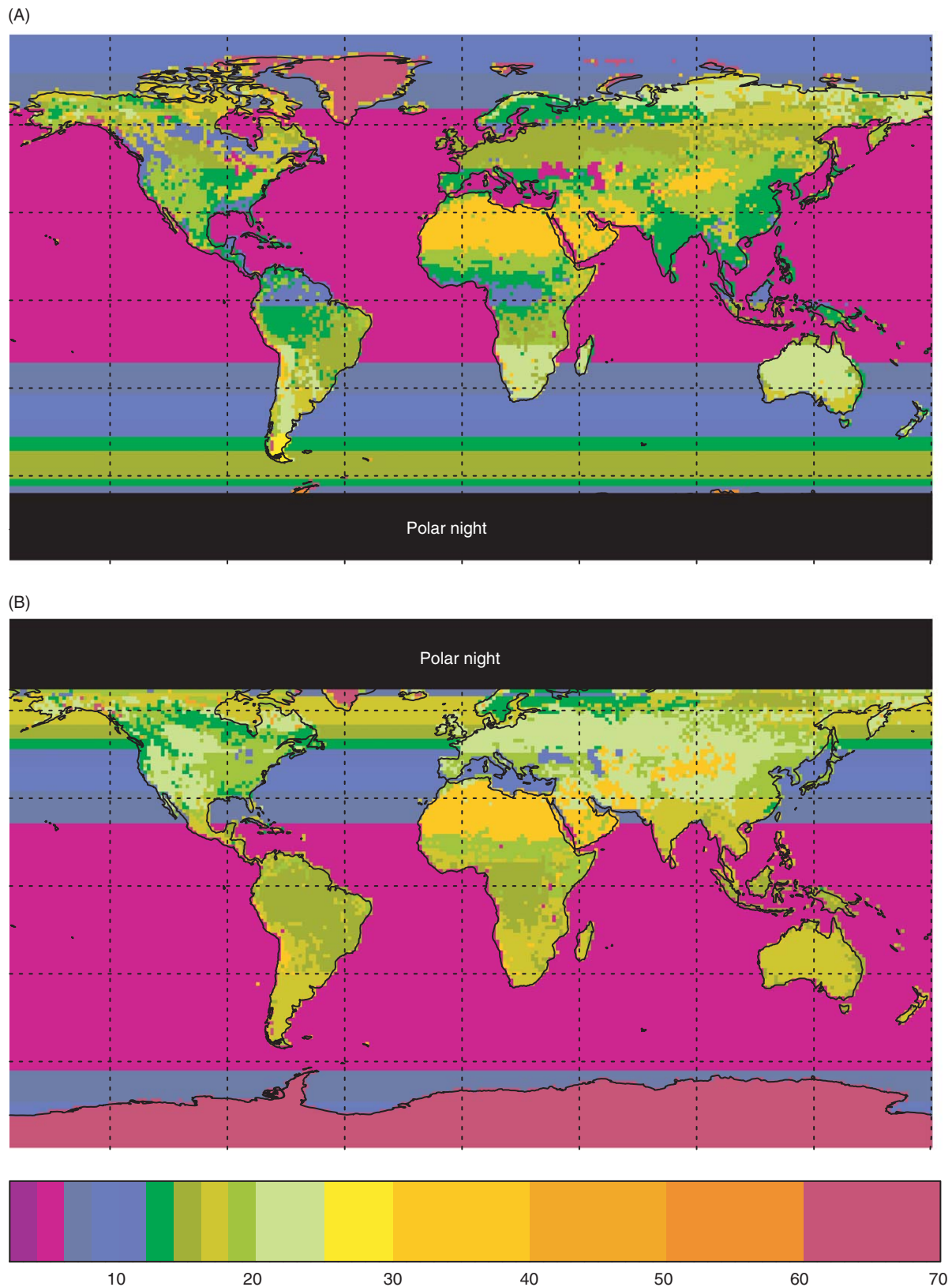
Figure 4 Maps of diurnally averaged surface albedos under cloud-free conditions for Northern Hemisphere summer (A) and Northern Hemisphere winter (B) solstices derived using an inventory of surface types and eqns [2] and [9]–[11], with values of the spectral albedos, solar zenith angle correction factor, d, and fraction covered by primary surface type, f, from Briegleb *et al.* (1986) and Briegleb and Ramanathan (1982) as given in **Tables 2** and **3**. The maps do not include seasonal sea-ice or snow cover.

Values given in **Table 2**, along with eqns [2] and [9]–[11], have been used in combination with surface types to construct global maps of the diurnally averaged surface albedo for winter and summer solstice conditions under cloud-free skies. Such maps are shown in **Figure 4**. The albedos in the maps do not include the effects of seasonal snowfall, or year-round snow on elevated mountain ranges. For the estimates shown in **Figure 4**, atmospheric concentrations of water vapor and ozone were taken from climatologies for the tropics and for summer and winter conditions at middle and polar latitudes. In addition, an aerosol with a $0.55\,\mu m$ optical depth of 0.1 and having properties typical of a marine aerosol was used over oceans and a similar aerosol having properties typical of continents was used over land. The aerosols increased the diffuse radiation incident on the surface at the expense of the incident direct sunlight. Broadband albedos for a solar zenith of $60°$ based on these calculations are also given in **Table 3**.

The albedos shown in **Figure 4** reflect the effects of seasonal changes in vegetation, solar zenith angle, and through changes in the concentration of water vapor and ozone, the composition of the cloud-free atmosphere. It should be recognized that the values of surface albedos given in the figure and those in **Tables 2** and **3** should be considered as no more than reasonable estimates. Accurate values await the accumulation and analysis of global satellite observations like those discussed earlier.

Nomenclature

List of Symbols and Definitions

d	Adjustable parameter used to derive direct albedo from diffuse albedo, eqn [9].
$d\Omega$	Differential increment of solid angle.
$F^{\pm}$	Downward $(-)$, upward $(+)$ broadband radiative flux, all wavelengths included.
$F^{-}_{i\text{DIF}}$	Downward flux of diffuse sunlight in spectral interval i incident on surface. Diffuse sunlight is light that has been scattered into directions markedly different from that of direct sunlight.
$F^{-}_{i\text{DIR}}$	Downward flux of direct sunlight in spectral interval i incident on surface. Direct sunlight is light that passes through the atmosphere without suffering scattering or absorption.
$F^{\pm}_{\lambda}$	Downward $(-)$, upward $(+)$ flux of light with wavelength λ at the surface.
g	Asymmetry parameter. Average value of cosine of the scattering angle for scattered light, eqn [6].
$I^{\pm}_{\lambda}$ and $I^{\pm}_{\lambda}(\theta, \phi)$	Downward $(-)$, upward $(+)$ specific intensity, or radiance, with wavelength λ.
k	Adjustable parameter in empirical representation of BRDF, eqn [7].
$P(g, \Theta)$	Henyey–Greenstein phase function, eqn [5].
$P(\Theta)$	Probability distribution function, or scattering phase function, for scattering at angle Θ. Fraction of light scattered per unit solid angle at scattering angle Θ between Θ and $\Theta + d\Theta$ into incremental ring of solid angle given by $2\pi \sin \Theta \, d\Theta$.
$R(G, \Delta)$	Correction factor for 'hot-spot', eqn [8].
$R_{i\text{D}}$	Spherical albedo for atmosphere in wavelength interval i when viewed from the surface. The spherical albedo is the albedo for diffuse incident radiation.
α	Broadband albedo, or simply albedo. Fraction of light reflected, all wavelengths of the incident light included.
$\alpha_i(\mu_0)$	Albedo for direct sunlight in spectral interval i, incident on the surface with solar zenith angle for which the cosine is μ_0.
$\alpha_{i\text{D}}$	Albedo for diffuse sunlight in spectral interval i.
α_{λ}	Spectral albedo. Fraction of light reflected at wavelength λ.
Δ	Adjustable parameter in correction for 'hot-spot', eqn [8].
θ	View zenith angle. The angle between the direction to the observer and the normal to the surface.
θ'	Zenith angle of incident sunlight that has been scattered in the atmosphere.
θ_0	Solar zenith angle. The angle between the direction to the sun and the normal to the surface.
Θ	Scattering angle. Angle between incident and scattered or reflected light.
λ	Wavelength of light.
μ_0	cosine of the solar zenith angle.
π	3.14159.
ρ_0	Adjustable parameter in empirical representation of BRDF, eqn [7].
$\rho(\theta', \theta, \phi)$	Bidirectional reflectance distribution function, eqn [7].
ϕ	Relative azimuth angle. The angle between the direction of the incident sunlight and the direction of the reflected light when projected in the plane containing the reflecting surface.
ϕ'	Relative azimuth angle of sunlight that has been scattered in the atmosphere.

See also

Aerosols: Climatology of Tropospheric Aerosols. **Agricultural Meteorology and Climatology**. **Air–Sea Interaction:** Sea Surface Temperature. **Antarctic Climate**. **Boundary Layers:** Surface Layer. **Deserts and Desertification**. **Land–Atmosphere Interactions:** Canopy Processes. **Optics, Atmospheric:** Optical Remote Sensing Instruments. **Radiative Transfer:** Scattering. **Satellite Remote Sensing:** Aerosol Measurements. **Sea Ice**. **Snow (Surface)**.

Further Reading

Bicheron P and Leroy M (2000) Bidirectional reflectance distribution function signatures of major biomes observed from space. *Journal of Geophysical Research* 105: 26669–26691.

Briegleb B and Ramanathan V (1982) Spectral and diurnal variations in clear sky planetary albedo. *Journal of Applied Meteorology* 21: 1160–1171.

Briegleb BP, Minnis P, Ramanathan V and Harrison E (1986) Comparison of regional clear-sky albedos inferred from satellite observations and model computations. *Journal of Climate and Applied Meteorology* 25: 214–226.

Dickenson RE (1983) Land surface processes and climate – surface albedos and energy budget. *Advances in Geophysics* 25: 305–353.

Goody RM and Yung YL (1989) *Atmospheric Radiation, Theoretical Basis*. New York: Oxford University Press.

Hartmann DL (1994) *Global Physical Climatology.* San Diego, CA: Academic Press.

Henderson-Sellers A and Wilson MF (1983) Surface albedo data for climate modeling. *Review of Geophysics and Space Physics* 21: 1743–1778.

Justice C, Vermote E, Townshend J, *et al*. (1998) The Moderate Resolution Imaging Spectroradiometer (MODIS): land remote sensing for global change research. *IEEE Transactions on Geoscience and Remote Sensing* 36: 1228–1249.

Lucht W, Hyman AH, Strahler AH, *et al*. (2000) A comparison of satellite-derived spectral albedos to ground-based broadband albedo measurements modeled to satellite spatial scale for a semidesert landscape. *Remote Sensing of the Environment* 74: 85–98.

Pinty B, Roveda F, Verstraete MM, *et al*. (2000) Surface albedo retrieval from Meteosat 2. Applications. *Journal of Geophysical Research* 105: 18113–18134.

Rahman H, Pinty B and Verstraete MM (1993) Coupled surface–atmosphere reflectance (CSAR) model 2. Semi-empirical surface model usable with NOAA Advanced Very High Resolution Radiometer data. *Journal of Geophysical Research* 98: 20791–20801.

Strugnell NC, Lucht W and Schaaf CB (2001) A global albedo data set derived from AVHRR data for use in climate simulations. *Geophysical Research Letters* 38: 191–194.

Thomas GE and Stamnes K (1999) *Radiative Transfer in the Atmosphere and Oceans*. New York: Cambridge University Press.

ROSSBY WAVES

P B Rhines, University of Washington, Seattle, WA, USA

Introduction

Large-scale undulations in the westerly winds are related to an ideal form of motion known as the 'Rossby' or 'planetary' wave. These waves owe their existence to the rotation and spherical shape of the Earth. Weather patterns and the general circulation are mostly much wider than the depth of the atmosphere: viewed from the side, a weather system is 100 to 1000 times thinner (vertically) than its width. This extreme thinness, beyond reminding us of the fragile nature of the atmosphere, causes horizontal winds to be stronger than vertical winds in such weather systems. Stable layering of the air, with its great variations in density, reinforce this inequality. Waves then become possible, which are dominated by nearly horizontal wind patterns, in many ways unlike the familiar waves on the sea or those of sound or light.

In their most general form, Rossby waves have an important bearing on what we call 'weather' and on the form of the general circulation of the Earth's atmosphere and its oceans, and on the atmospheres of other planets. Indeed, the form of the general circulation is in part shaped by Rossby waves. In their most general form, Rossby waves occur widely in fluid flows of many kinds (for example, in hurricanes). To understand these waves completely requires a challenging amount of mathematics and physics, but many of their properties can nevertheless be appreciated through ideas, observations, and experiments that could be found in a high-school physics course. Because the language of science can be artificially complex, we provide translations of some unfamiliar terms inside brackets { }. Some mathematical equations are included, but these can be skipped by those unfamiliar with them.